

Laser Assisted Collisions of Electrons with Metal Vapours*

P. J. O. Teubner, P. M. Farrell,^A V. Karaganov, M. R. Law and V. Suvorov

Department of Physics, Flinders University of South Australia,
GPO Box 2100, Bedford Park, SA 5001, Australia.

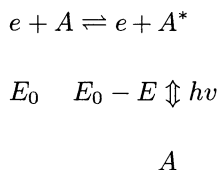
^A Department of Applied Physics, Victoria University of Technology,
GPO Box 14428, MMC Melbourne, Vic. 3000, Australia.

Abstract

Three separate experiments are described which use laser radiation to probe the details of electron scattering processes from metal vapour targets. Results from superelastic scattering experiments from calcium are presented. The experiments were carried out at incident energies of 25.7 and 45 eV referred to the ground state. Scattering amplitudes derived from these experiments demonstrate that current theories are inadequate. The coherence of the excitation process has been studied by measuring the total polarisation. It is shown that the excitation process is coherent over the whole kinematic range. Preliminary results from a study of superelastic electron scattering from lithium are discussed where it is shown that a quantum electrodynamical model can be used to describe the optical pumping process in ⁶Li and ⁷Li. In addition the first superelastic electron spectrum is presented for experiments on lithium. A stepwise excitation technique is described with which cross sections for the electron impact excitation of the 3d⁹4s² ²D state in copper can be measured. The experiments are complicated by the presence of D states in the incident copper beam. The origin of these D states is described as is a modification of the technique which leads to their removal.

1. Introduction

Macek and Jaecks (1971) observed that electron scattering experiments in which the scattered electron and the decay photon were detected in coincidence could provide information about the magnitude and phase of the scattering amplitudes which describe the collision process. In these experiments an electron of energy E_0 excites a state of an excitation energy E in a target atom A. The electron is scattered with energy $E_0 - E$ leaving the atom in an excited state that subsequently emits a photon of energy E :



* Refereed paper based on a contribution to the Advanced Workshop on Atomic and Molecular Physics, held at the Australian National University, Canberra, in February 1995.

Hertel and Stoll (1974) recognised that this process was reversible. In this case a ground state atom is excited by laser radiation to an excited state and interacts with electrons of energy $E_0 - E$. Electrons which gain energy in the collision, that is with energy E_0 , are detected. This technique is called superelastic scattering and has the advantage over the coincidence technique in that single electrons are detected. The polarisation of the electromagnetic radiation is given by that of the laser beam. Given that the coincidence technique in electron scattering from metal vapours is in general restricted to scattering angles of less than 15° , and that differential cross sections for inelastic scattering from metals are strongly peaked in the forward direction, it is not surprising that the superelastic technique has found its most widespread use in electron scattering from metal vapours. The details of this technique have been reviewed extensively by Andersen *et al.* (1988).

The other type of experiment that we discuss in this paper uses the stepwise excitation technique. This technique is particularly suitable in the study of electron impact excitation of low lying metastable states that are difficult to detect by conventional techniques. The basic features of the technique are shown in Fig. 1. The metastable state $|2\rangle$ is excited by electron impact from state $|1\rangle$. A laser is tuned to an appropriate wavelength to excite state $|3\rangle$ from state $|2\rangle$. State $|3\rangle$ then fluoresces to the ground state. The fluorescent radiation is detected and its intensity is proportional to the number of atoms in state $|2\rangle$.

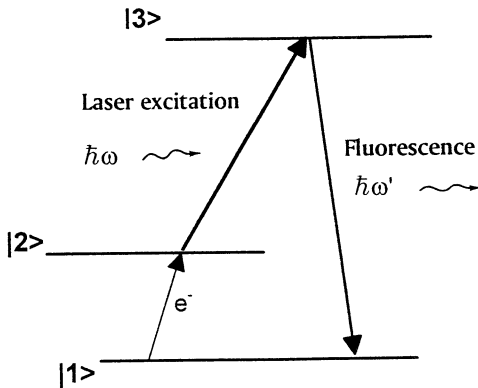


Fig. 1. Schematic diagram of the stepwise technique.

2. Superelastic Scattering Experiments

In these experiments electrons are scattered from the excited state of an atom which has been prepared by optical pumping with laser radiation from the ground state. Electrons are detected which have gained energy from the excited state equal to the difference in energy between the excited state and the ground state. Fig. 2 shows a schematic diagram of the typical apparatus for a superelastic scattering experiment. Details of the actual experiment are given by Law and Teubner (1995). An energy analyser views the region where the atomic, electron and laser beams overlap and it analyses the energy of the electrons scattered at a particular scattering angle. Fig. 3 shows a typical spectrum from such an experiment. The superelastic peak is clearly identified on the right of the spectrum. In this case the target was calcium, the incident energy of the electrons

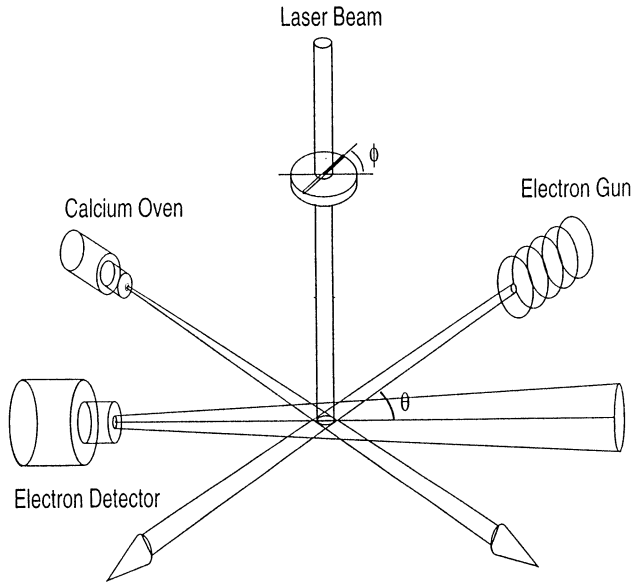


Fig. 2. Schematic diagram of the apparatus used in superelastic scattering experiments from optically pumped calcium atoms.

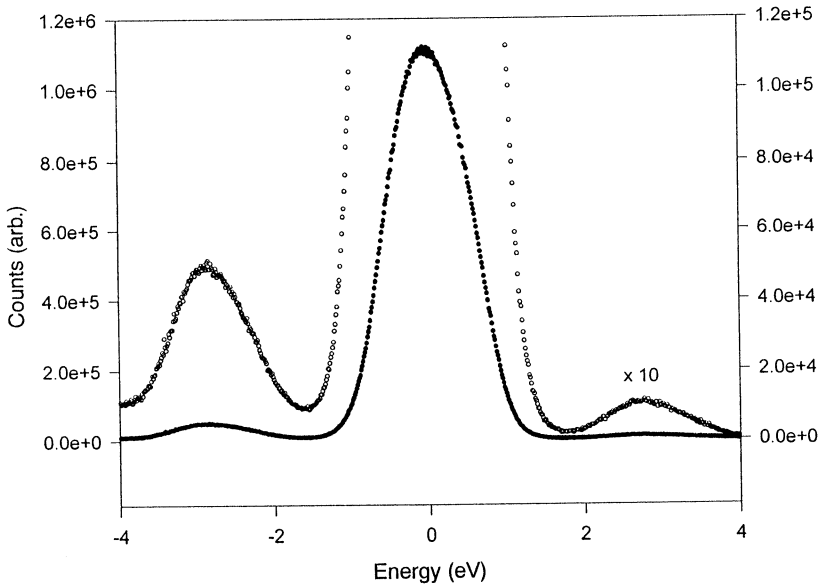


Fig. 3. Typical energy loss/gain spectrum taken in a superelastic scattering experiment from calcium. The incident electron energy was 40 eV and the electron scattering angle was 10° .

was 40 eV and the scattering angle was 10° . The experiments are conducted by measuring the superelastic signal as a function of the polarisation of the laser beam. From this one can define the equivalent Stokes parameters for the collision:

$$P_1 = \frac{I(0) - I(90)}{I(0) + I(90)}, \quad (1)$$

$$P_2 = \frac{I(45) - I(135)}{I(45) + I(135)}, \quad (2)$$

$$P_3 = \frac{I(RHC) - I(LHC)}{I(RHC) + I(LHC)}, \quad (3)$$

where $I(\alpha)$ is the number of superelastically scattered electrons when the incident laser beam is polarised at α° to the outgoing electron direction.

Andersen *et al.* (1988) have shown that the final state wavefunction $|\Psi\rangle$ for the excitation of a P state can be represented in the natural coordinate frame as

$$|\Psi\rangle = a_1 |1\rangle + a_{-1} |-1\rangle,$$

where the a_m are the scattering amplitudes for the excitation of the magnetic substates m_L .

The components of the Stokes vector are related to the amplitudes a_1 , a_{-1} in equation (1) by

$$P_1 = -2\text{Re } a_1 a_{-1}^*, \quad (5)$$

$$P_2 = 2\text{Im } a_1 a_{-1}^*, \quad (6)$$

$$P_3 = |a_1|^2 - |a_{-1}|^2, \quad (7)$$

where we have ignored possible spin dependent processes in the collision. This approach is valid for singlet to singlet transitions such as apply in atoms where LS coupling can be used to high accuracy in describing the two states involved in the collision. This is expected to be the case for collisions with the 4^1P state in calcium. In the case of collisions with lithium, where spin cannot be neglected, it is necessary to define scattering amplitudes a_1 and a_{-1} for the singlet and for the triplet channels. In our experiments we do not distinguish the spin of either the electrons or atoms so in this case one must average over the spin states. The ways in which equations (5), (6) and (7) are altered in this case are given by Andersen *et al.* (1988).

The scattering amplitudes a together with the bound state wavefunctions fully characterise the final state wavefunction. Its shape and its alignment in the scattering plane is shown schematically in Fig. 4. In the natural coordinate frame the incident electron beam is parallel to the x axis; the scattering plane is the xy plane and the laser beam is introduced along the z axis. The alignment angle γ is related to equations (2) and (3) by

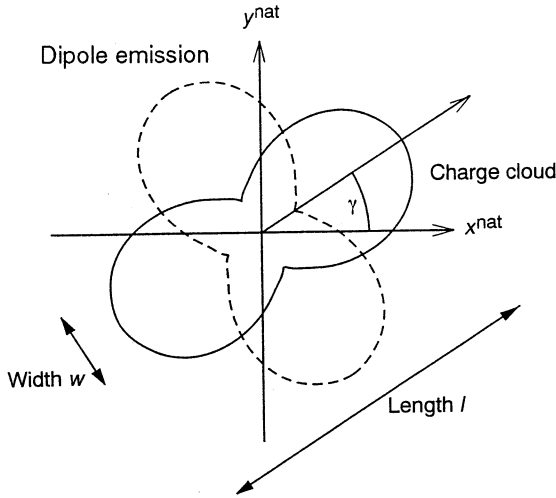


Fig. 4. Schematic diagram of a section of the charge cloud distribution in the electron impact excitation of a P state showing the alignment angle γ .

$$\gamma = \frac{1}{2} \arg(P_1 + i P_2). \tag{8}$$

The total linear polarisation

$$P_l = [P_1^2 + P_2^2]^2 \tag{9}$$

and the relative width w and length l of the charge cloud is found from

$$l = \frac{1 + P_l}{2}, \tag{10}$$

$$w = \frac{1 - P_l}{2}. \tag{11}$$

The angular momentum transferred normal to the scattering plane L_\perp is given by

$$L_\perp = -P_3.$$

The coherence of the excitation process can be determined from the frame independent coherence parameter P^+ where

$$P^+ = [P_1^2 + P_2^2 + P_3^2]^{\frac{1}{2}}. \tag{12}$$

(2a) Calcium

Calcium is a closed shell atom in which the ground 4S state and excited P state can both be described by LS coupling to quite high accuracy (Kuhn 1969).

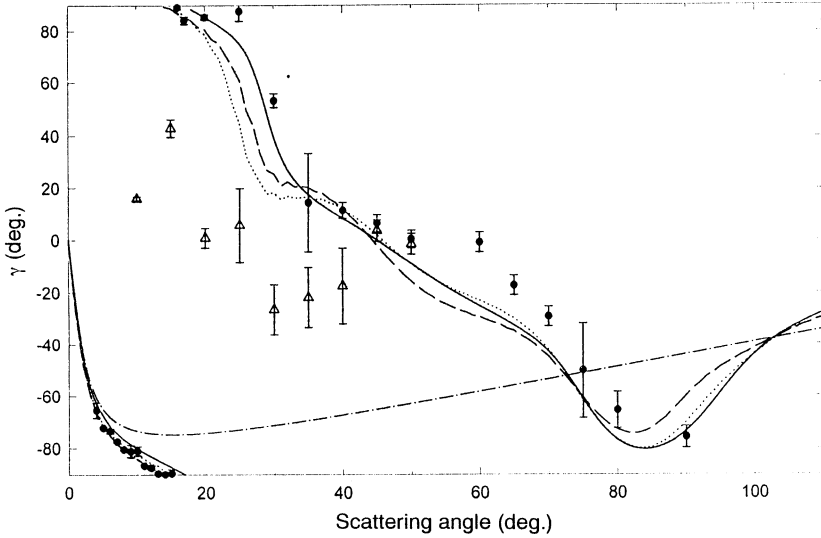


Fig. 5. Parameter γ as a function of the electron scattering angle at an energy of 45 eV referred to the ground state. The present results (\bullet) are compared with the theoretical predictions of the distorted wave theories of Srivastava *et al.* (1992) (—), with the FOMBT of Clark *et al.* (1994) (\cdots) and with the DWA (---). The Born approximation predictions are shown also (- · - ·). The results of the coincidence experiment of El-Fayoum *et al.* (1989) are shown (\blacktriangle).

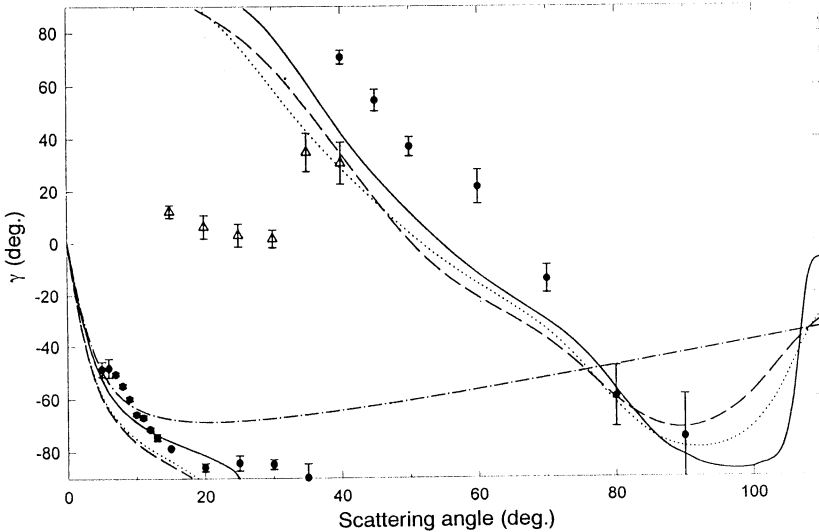


Fig. 6. Parameter γ as a function of the electron scattering angle at an energy of 25.7 eV. The legend is as for Fig. 5.

Thus the 4S–4P transition can be accurately described as a singlet to singlet transition so we can predict that the excitation will be coherent and P^+ should be unity. The P state is also strongly coupled to the S state so it offers some of the advantages in the description of the scattering problem that have been known for many years in the electron–sodium problem (Moore and Norcross 1972). The calcium atom is accessible to optical pumping techniques with a

commercial dye laser because the resonance P-S transition has a wavelength *in vacuo* of 422.79 nm. Laser radiation can be produced at appropriate power levels with some difficulty by pumping the dye Stilbene 3 with UV light. Three different distorted wave calculations have been performed on the electron impact excitation of the 4^1P state in calcium; a first order many body theory calculation by Clark and Csanak (Clark *et al.* 1989), a relativistic distorted wave calculation by Srivastava *et al.* (1992) and a distorted wave calculation by Clark (1994).

In Fig. 5 we show our measurements of the parameter γ taken at an incident electron energy of 45 eV compared to the predictions of several theories. The error bars represent plus and minus one standard deviation. The alignment angles predicted by the first Born approximation are clearly inadequate at all but the most forward angles. Although there are significant differences between the three more sophisticated theories, the experimental results favour none of them over the whole angular range. All theories predict the change of quadrant at about 15° which is confirmed by the experiments. The overall agreement in shape between the theories and the experiment is good. The distorted wave theory of Clark (1994) is excellent out to 20° .

The situation is not as promising at an incident energy of 25.7 eV which is shown in Fig. 6. Here there is a very large difference between theory and experiment at the change of quadrant and the theories in this case do not predict the alignment angle even at the most forward angles. It is clear that 25.7 eV is too low in energy for distorted wave theories to be used. This is confirmed in Fig. 7 where we show the angular momentum transferred normal to the scattering plane L_\perp as a function of the electron scattering angle. In this case the RDWA calculation of Srivastava *et al.* (1992) adequately describes the collision at small scattering angles, but it breaks down for scattering angles greater than about 20° . The electron-photon coincidence measurements of the

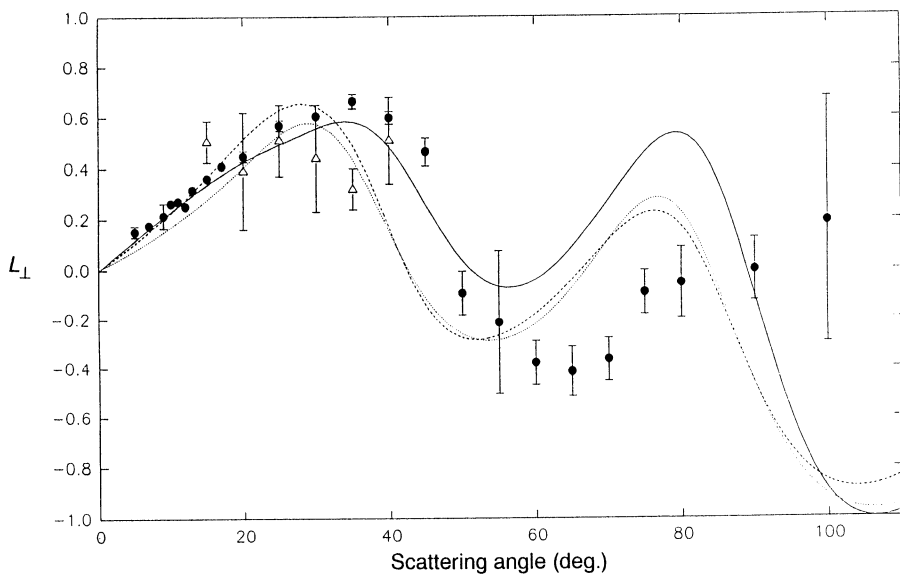


Fig. 7. Orientation parameter L_\perp as a function of the electron scattering angle. The incident electron energy is 25.7 eV. The legend is as for Fig. 5.

Stirling group (El-Fayoumi *et al.* 1988) which are the time reversed equivalent of the present work are also shown. Agreement between the two experiments is poor even though the uncertainties in the coincidence data are very large.

Fig. 8 shows the parameter P^+ as a function of the electron scattering angle at an incident energy of 45 eV. The data show that $P^+ = 1$ within experimental error over the whole angular range. This confirms the proposition of Blum (1981) that the scattering amplitudes for the excitation of singlet states will be independent of the spin. Thus the excitation will be coherent and $P^+ = 1$. Although they are not shown in Fig. 8, all theories predict $P^+ = 1$ which is a consequence of the fact that they all used an LS coupled basis to describe the bound states. The present results do not support the apparent loss of coherence that was observed in the coincidence experiments (Zohny *et al.* 1989) at around 20° .

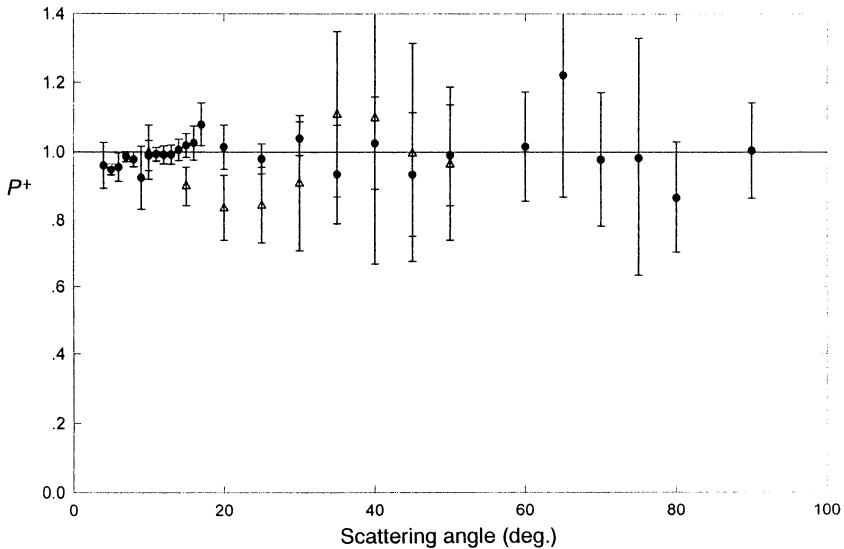


Fig. 8. Parameter P^+ as a function of the electron scattering angle for an incident electron energy of 45 eV. The coincidence results of Zohny *et al.* (1989) are shown as (\blacktriangle).

These results show that there is scope for the application of other scattering models to predict scattering parameters for electron scattering from calcium. Although the presence of D states close to the P state makes the description of the bound states in calcium far more complicated than it is in say sodium, it would appear that convergent coupled channels calculation can be used profitably in this case.

(2b) Lithium

The success of the convergent coupled channels theory of Bray (1994) in predicting orientation and alignment parameters in electron collisions with sodium prompts the question of how good is this theory in describing scattering from other open shell atoms. Of course the ultimate test rests with the description of electron scattering from atomic hydrogen. It is not possible to perform superelastic scattering experiments on atomic hydrogen so the next best target

is lithium. Lithium has the advantage over sodium that the wavefunctions are known more accurately and it is a much better target to test the scattering theory than sodium because the coupling between the ground state and first excited state is weaker in lithium than for sodium.

The 2^2P to 2^2S transition in lithium has a wavelength in the red for both isotopes ^7Li and ^6Li . This wavelength can be achieved by pumping the dye DCM with green light. The problem of achieving significant excited state population in optically pumped lithium is demonstrated in Fig. 9 where we compare the hyperfine (HF) splitting of both lithium isotopes with that in ^{23}Na . The standard technique used to pump ^{23}Na optically is to tune the laser to the $\bar{F}=2$ level in the ground state to the $F=3$ level in the $3P_{3/2}$. Notwithstanding the saturation broadening of this line to about 70 MHz it is possible to prepare sizable excited state populations using linearly polarised light. The difficulties of using single frequency pumping in either of the lithium isotopes are then apparent. The natural width of the hyperfine structure states is comparable to the HFS separation, so intuitively one would predict that it is impossible to pump lithium with single frequency laser radiation. This observation led Baum *et al.* (1980) to use an acousto-optic modulator to prepare aligned lithium atoms in their work on scattering asymmetries in electron scattering from lithium.

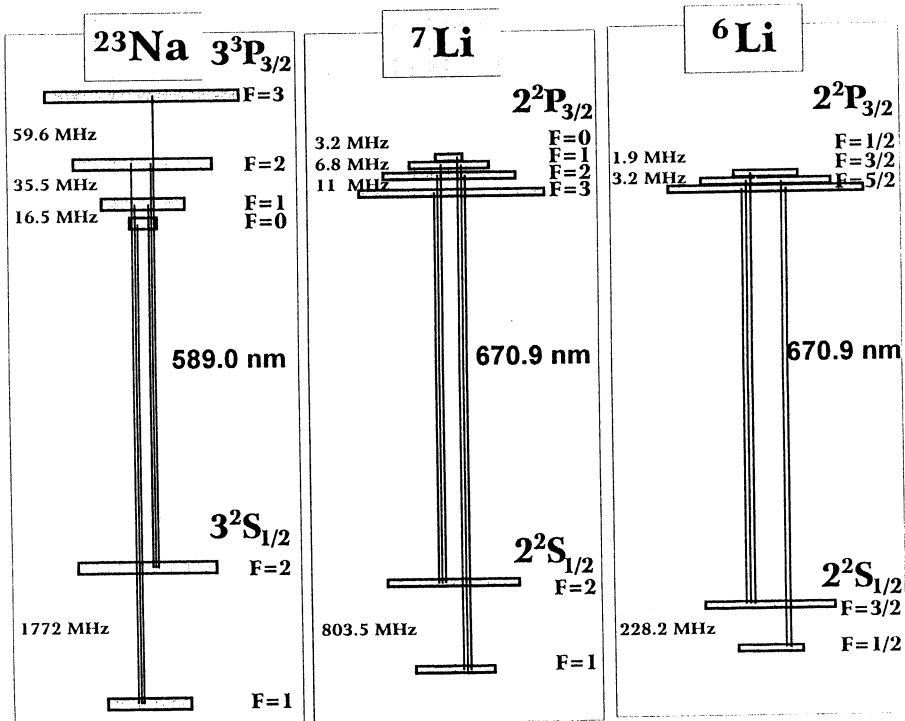


Fig. 9. HF splitting of the ground and first excited states of ^{23}Na , ^6Li and ^7Li .

A more detailed study of the optical pumping process shows that it is possible to achieve excited state population using single frequency light. These calculations have used Heisenberg atomic operators in the quantum electrodynamical model that was developed by Farrell *et al.* (1988) to predict the intensity and polarisation

of the decay radiation when laser radiation is incident on lithium atoms. The model has been modified to permit excitation from both HF levels of the ground state. In the sodium case this was neglected. However, in the case of lithium, off-diagonal elements that describe coherences between ground states with the same m_F but different F must be included.

There are no free parameters in these models. The parameters required for input are the lifetime of the excited state, HF splittings of the ground $2^2S_{1/2}$ state and the $2^2P_{3/2}$ state, the laser intensity, the Doppler width of the atomic beam and the quantum numbers. All of these parameters are either well known or they can be measured. We are in the process of testing the validity of the predictions of the model but preliminary results are very encouraging. For example in Fig. 10a we compare the fluorescence intensity emitted by ^7Li normal to the direction of the laser beam as a function of the laser power. The laser power has been varied over four orders of magnitude. The two sets of data shown in Fig. 10a arise from two different runs and indicate the reproducibility of the results. In Fig. 10b we compare the polarisation of the fluorescence radiation with the laser power. Again there is good agreement between the experimental results and the predictions of the theory.

The question now is: can we improve the excited state polarisation by pumping with two frequencies? To answer this question we have tried two different techniques which permit two frequency pumping of the ground state levels. The first is illustrated schematically in Fig. 11 and uses a counter propagating technique reported by Carster *et al.* (1975). In this method the lithium beam is inclined at some angle θ to the laser beam. The laser beam is reflected back on itself by a mirror. The frequency of the forward laser beam is Doppler shifted toward the red by

$$\nu_f = \nu_0 - v_a \frac{\cos\theta}{\lambda_0}, \quad (13)$$

where v_a is the average velocity of the ^7Li atoms, in our case 2000 m s^{-1} . The return laser beam is shifted towards the blue

$$\nu_r = \nu_0 + v_a \frac{\cos\theta}{\lambda_0}. \quad (14)$$

Thus the frequency difference of the two beams is

$$\Delta\nu = \nu_f - \nu_r = 2 v_a \frac{\cos\theta}{\lambda_0}. \quad (15)$$

For two frequency pumping of ^7Li , $\Delta\nu = 804 \text{ MHz}$. The single frequency laser beam has $\lambda_0 = 670.977 \text{ nm}$ thus an angle of $\theta = 81^\circ$ is required to pump the ^7Li . This implies that the lithium source must be tilted by 9° out of the horizontal plane. This probably precludes the use of this technique to determine scattering amplitudes. The influence of the mirror on circularly polarised radiation introduces serious complications on the measurement of P_3 but, nevertheless, it is possible to enhance the excited state population using this Doppler technique.

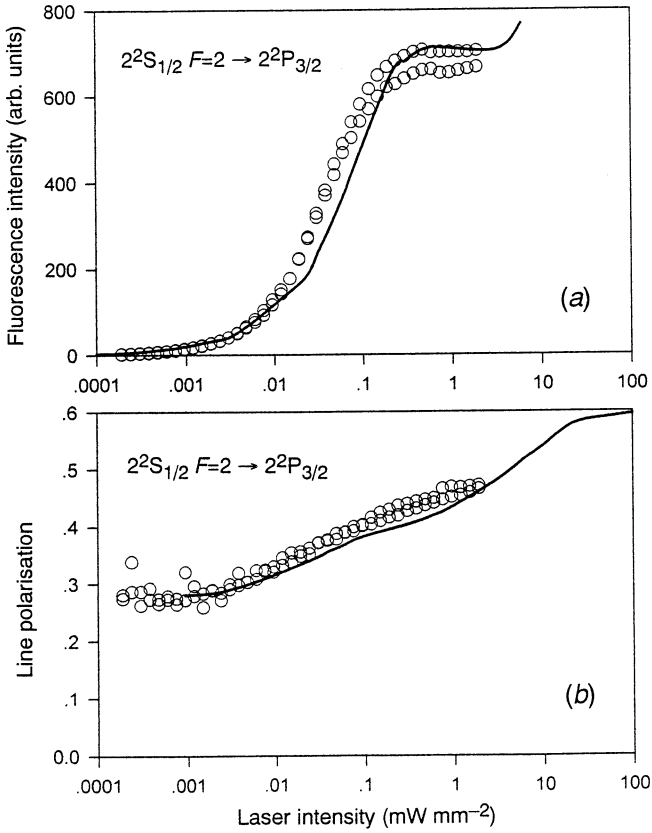


Fig. 10. Fluorescence intensity emitted by ${}^7\text{Li}$ normal to the laser beam direction as a function of the laser power. The experimental points are shown (\circ) and the predictions of the model ($-$) are shown. (b) Polarisation of the fluorescent radiation emitted by ${}^7\text{Li}$ as a function of the laser power. The experimental points (\circ) and the theoretical predictions ($-$) are shown.

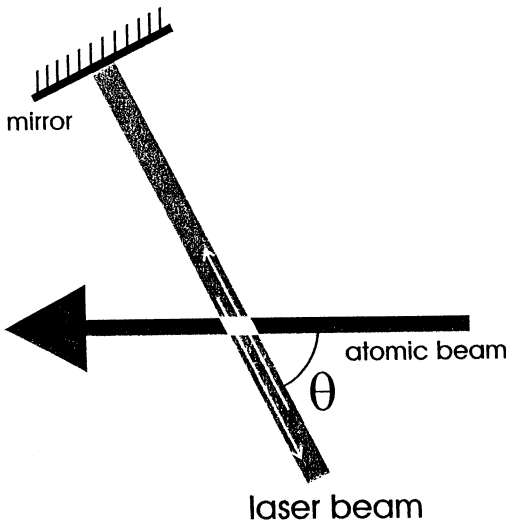


Fig. 11. Schematic diagram of a counter propagating technique used to pump both ground state levels of ${}^7\text{Li}$.

This fact can be ascertained by the data shown in Fig. 12 which shows an energy loss/gain spectrum for the scattering of 20 eV electrons from optically pumped ${}^7\text{Li}$ atoms at a scattering angle of 10° . The Doppler technique was used in this case. The presence of the superelastic peak at the right of the peak is immediately obvious. The data in this figure represent the first observation of superelastic electron scattering from lithium.

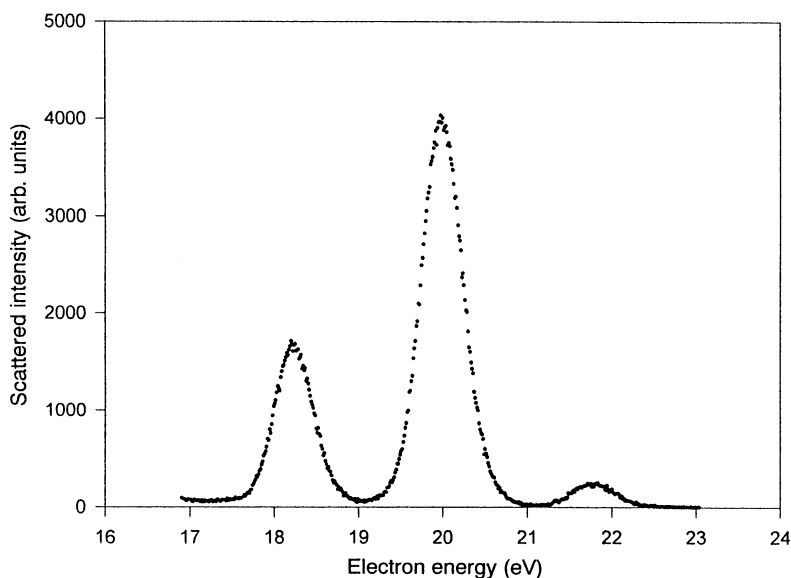


Fig. 12. Energy loss/gain spectrum of electrons scattered from optically pumped lithium atoms. The incident energy was 20 eV and the scattering angle 10° .

In principle the problems associated with the technique can be resolved by converting single frequency laser radiation into multifrequency light by using an electro-optical modulator (EOM) (Kelly and Gallagher 1987). Here a single frequency laser beam passes through a LiTaO_3 crystal which is coupled to an RF generator through a tuned LC circuit. The generator delivers half the frequency separation of the HF splitting in the ground state; that is 402 MHz for ${}^7\text{Li}$ and 114 MHz for ${}^6\text{Li}$. Optical pumping experiments using this technique have been carried out on both ${}^6\text{Li}$ and ${}^7\text{Li}$ and we have observed significantly enhanced fluorescence from the excited lithium beams. We anticipate that we will use this technique for the superelastic scattering experiments once we have resolved the problems of stability associated with the modulating crystal. We have explored the possibility of using an acousto-optic modulator (AOM) to introduce the relevant sidebands. It transpires that the EOM has significant cost benefit over the AOM, specifically in work with ${}^7\text{Li}$ but also with ${}^6\text{Li}$.

3. Stepwise Excitation Experiments

These experiments allow the detection of metastable states which are either inaccessible or difficult to detect by other means. In this case we are studying the electron impact excitation of the $3d^94s^2\ 2D$ state in copper. This state is the

lower level in the lasing process of the copper vapour laser. Cross sections for the excitation of this state are therefore very important for models of the laser. Very little is known about these cross sections. The only experimental information is that by Trajmar *et al.* (1977) who measured a series of angular distributions for the excitation of this state at electron impact energies of 6, 20 and 60 eV. These relative cross sections were normalised to elastic scattering cross sections which were in turn normalised to a static exchange calculation of Winter (1977, cited in Trajmar *et al.* 1977) for elastic scattering at 100 eV and 40° . It is now well established (Ismail and Teubner 1995) that the theory overestimated the cross section by a factor of about 7. Trajmar *et al.* made no measurements below 15° so, as well as the problems with normalisation, there may be problems with the integral cross sections that they deduced from their angular distributions.

Scheibner *et al.* (1987) have used a close coupling theory to predict the excitation of the 2D state by electron impact. They predicted a broad resonance at about 2.5 eV where the cross section is enhanced by a factor of 7 over the cross section at 6 eV. There clearly is a need for further experimental studies of this cross section, not only at 6 eV where the work of Trajmar *et al.* can be tested, but also at energies close to threshold where the predictions of the close coupling theory can be tested.

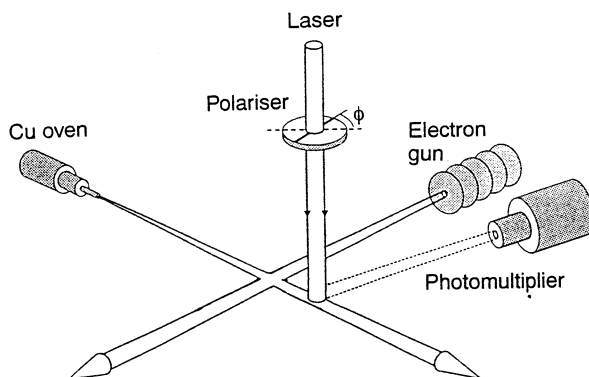


Fig. 13. Schematic diagram of the apparatus used to study the excitation of the D states in copper.

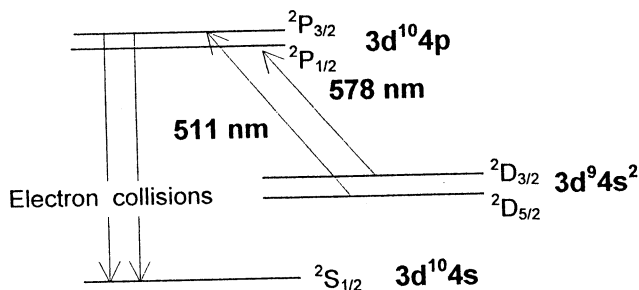


Fig. 14. Energy level diagram of the first three states in copper.

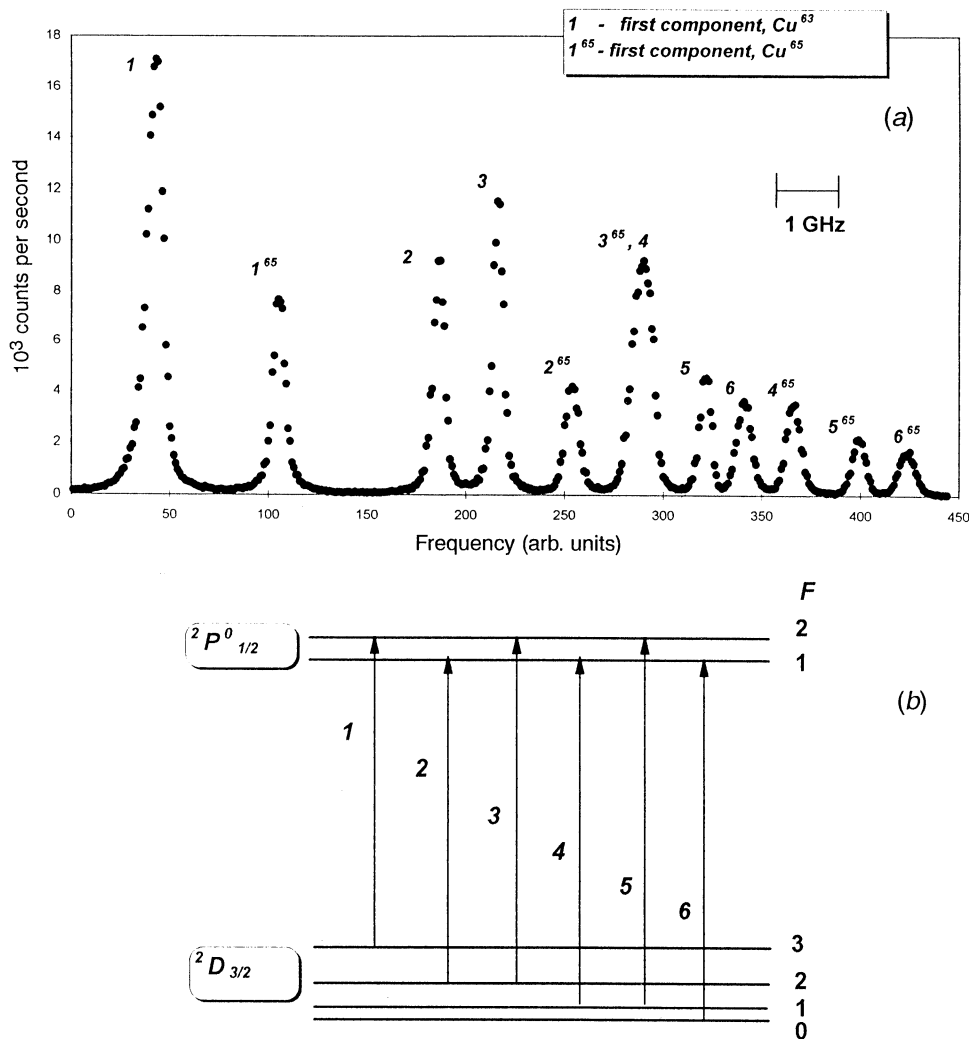


Fig. 15. (a) Fluorescence spectrum from the $3d^94s^2\ ^2D_{3/2}$ state in copper as the laser frequency is changed. (b) Hyperfine structure of the relevant levels in copper. The numbers refer to the origin of the lines in (a).

We have chosen a stepwise excitation technique to carry out these experiments. The basic features of the technique are shown in Fig. 13. A beam of copper atoms is excited by electrons in an interaction region. The electrons excite the metastable 2D state as well as other states principally the $3d^{10}4p\ ^2P$ state which decays with a lifetime 7.3 ns. Downstream from the interaction region the copper beam contains ground state atoms together with the 2D states that have been excited by electrons. Laser radiation is tuned to the D to P transition and the atoms decay to the ground state emitting 328 nm photons which are detected in a photomultiplier tube. The number of photons detected when the laser beam is on is a measure of the population of the D states.

The energy level diagram of the first three states of copper shown in Fig. 14 shows that there are two possible wavelengths for this technique, 511 and 578 nm.

We have chosen to probe the ${}^2D_{3/2}$ state with 578 nm radiation because of the relative ease of producing the appropriate wavelength with R6G dye. Our early attempts to use this technique were frustrated by the presence of D-state atoms in the copper beam before they reached the interaction region. Fig. 15a shows a spectrum of the count rate observed in the photomultiplier tube as the frequency of the laser is changed over a range of approximately 30 GHz. The richness of the spectrum arises from the HF splitting in the ${}^2P_{1/2}$ state and the ${}^2D_{3/2}$ state for both the isotopes ${}^{63}\text{Cu}$ and ${}^{65}\text{Cu}$. The origin of the numbers associated with each peak is shown in Fig. 15b.

We have identified the source of these D states as being due to the Boltzmann distribution of D-state atoms in the oven. At a given source temperature T the number of D-state atoms is given by

$$N_D = N_S e^{-(\Delta E/k T)}, \quad (16)$$

where ΔE is the energy of the $D_{3/2}$ state, k is Boltzmann constant and N_S is the number of ground state atoms. In our case

$$N_D = N_S e^{-(19056/T)}. \quad (17)$$

The number of ground state atoms depends on the pressure in the source which in turn depends exponentially on the inverse temperature

$$N_S = A e^{-(C_2/T)}, \quad (18)$$

where A and C_2 are constants. Therefore we get

$$N_D = A e^{-(C_2+19056/T)} = A e^{-(C/T)}. \quad (19)$$

We have determined the constant C_2 by observing the decay photons from the excitation of the 2P state by electron impact. This is shown in Fig. 16 where we plot the natural logarithm of the signal against the parameter $1/T$. We also show the variation of the D-state signal as a function of $1/T$. It is clear that the temperature variation of the D-state signal is consistent with that predicted by equation (19) and that $C = 50049$ from our measurements. The measured value of C_2 was 33134 so the predicted value is $C = 33134 + 19056 = 52190$. The difference between the two numbers of 4 % can be accounted for by uncertainties in the source temperature and statistical uncertainties. We are confident that we have identified the origin of the D-state atoms in the beam. Furthermore this residual signal is far greater than that which we expect from electron impact processes, so we are faced with the problem of removing the residual D-state atoms from the beam. The most obvious way of depleting the D state population before the interaction region is to employ the experimental geometry shown in Fig. 17. We expect that we would deplete the D-state population at the centre of the line in the manner shown in Fig. 18a which shows a detuning curve using the arrangement indicated in Fig. 17. It is clear that the population does not go to zero at the centre of the line. This phenomenon can be understood with the aid of rate equation calculations which we have carried out. These show

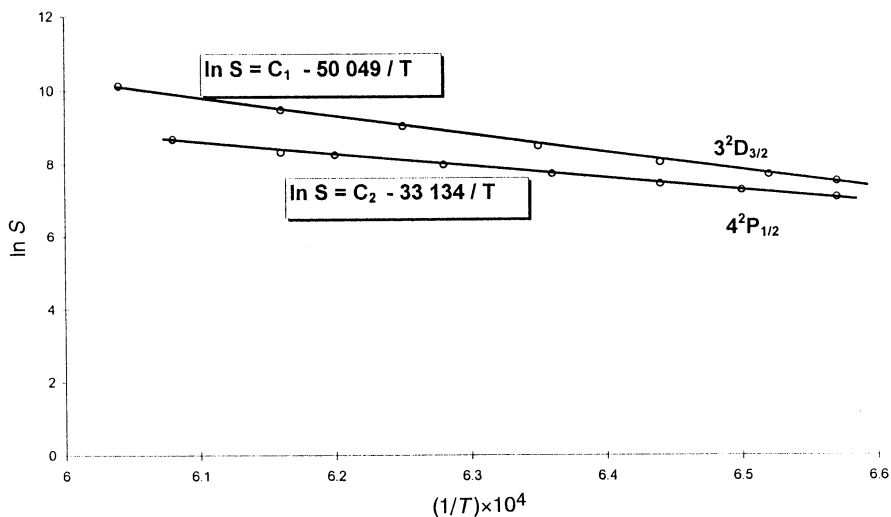


Fig. 16. Variation of the laser induced fluorescence signal as a function of T^{-1} where T is the temperature of the copper beam. Also shown is the variation of the signal derived from the excitation of the P states.

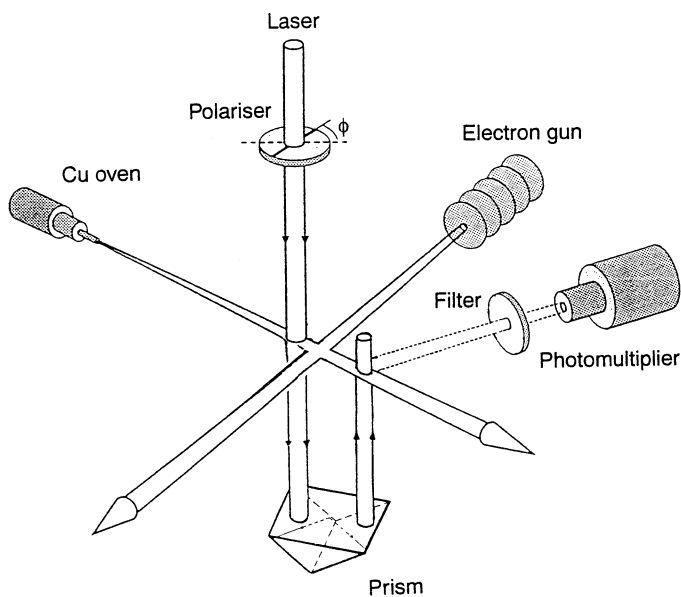


Fig. 17. Schematic diagram of the experimental geometry used to remove D states from the incident copper beam.

that the depth of the hole which is produced in the peak, or an equivalent Lamb dip, depends on the laser power and the initial and final HFS states in the spectrum. For example at a laser power of 300 mW the rate equations predict that about half of the D-state population will be removed from the line centre. This is consistent with the data shown in Fig. 18a. On the other hand in line 6 for ^{65}Cu about 93% of the D states will be removed from the centre of the line. Again this is consistent with our observations which are shown in

Fig. 18*b*. Therefore we are concentrating our study on line 6 and we can report that we have observed electron initiated D-state signals at an incident energy of 3 eV. These measurements indicate, however, that we must modulate the electron beam. Given the fact that we also chop the laser beam, this experiment which seemed to be so straightforward when we started has now become very complex.

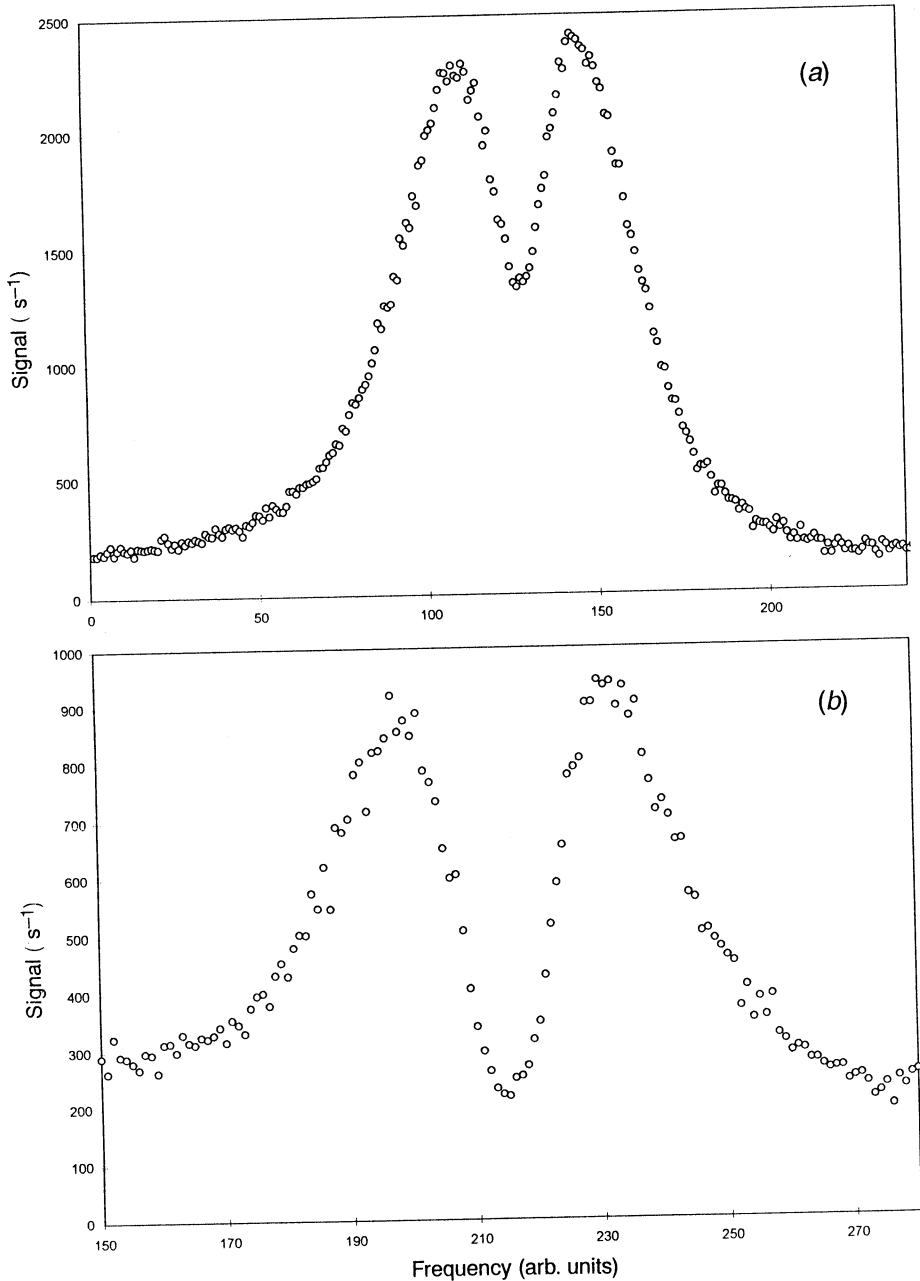


Fig. 18. Signal observed in (a) line 3 and (b) line 6 as a function of the laser frequency when the arrangement shown in Fig. 17 is used.

4. Conclusions

The work that we have reported on scattering parameters in calcium demonstrates that current distorted wave theories are inadequate at low energies. With complex atomic targets it is difficult to identify whether the problem with the theories lies in the scattering theory or in the wavefunctions. In this case the improvement in the predictions of the theories at 45 eV over those at 25.7 eV indicates that the wavefunctions used were of higher quality than the approximations used in the theory. Thus there is a clear need to apply close coupling calculations to this problem. Our work on lithium has demonstrated that it is possible to determine scattering parameters from superelastic scattering experiments on this target and we foreshadow that results from this project will be available soon. The stepwise excitation experiments in copper have been complicated by the presence of D states in our copper beam, but we have been able to demonstrate that this technique can produce D state cross sections at energies up to the threshold of the P state.

Acknowledgment

This research was supported by grants from the Australian Research Council.

References

- Andersen, N., Gallagher, J. W., and Hertel, I.V. (1988). *Phys. Rep.* **165**, 1.
- Baum, G., Caldwell, C. D., and Schröder, W. (1980). *App. Phys.* **21**, 121.
- Blum, K. (1981). 'Density Matrix Theory and Applications' (Plenum: New York).
- Bray, I. (1994). *Phys. Rev. A* **49**, 1066.
- Carter, G. M., Pritchard, D. E., and Ducas, T. W. (1975). *App. Phys. Lett.* **27**, 498.
- Clark, R. E. H. (1994). Personal communication.
- Clark, R. E. H., Abdullah, Jr. J., Csanak, G., and Kramer, S. P. (1989). *Phys. Rev. A* **40**, 2935.
- El-Fayoumi, M. A. K., Beyer, H.-J., Shahin, F., Eid, Y. A., and Kleinpoppen, H. (1988). Proc. Eleventh ICAP, p. 173.
- Farrell, P. M., MacGillivray, W. R., and Standage, M. C. (1988). *Phys. Rev. A* **37**, 4240.
- Hertel, I. V., and Stoll, W. (1974). *J. Phys. B* **7**, 570.
- Ismail, M., and Teubner, P. J. O. (1995). *J. Phys. B* **28**, 4149.
- Kelly, J. F., and Gallagher, A. (1987) *Rev. Sci. Instrum.* **58**, 563.
- Kuhn, H. G. (1969). 'Atomic Spectra', 2nd edn (Longman: London).
- Law, M. R., and Teubner, P. J. O. (1995). *J. Phys. B* **28**, 2257.
- Macek, J., and Jaceks, D. H. (1971). *Phys. Rev. A* **4**, 2288.
- Moores, D. L., and Norcross, D. W. (1972). *J. Phys. B* **5**, 1482.
- Scheibner, K. F., Hazi, A. V., and Henry, R. J. W. (1987). *Phys. Rev. A* **35**, 4869.
- Srivastava, R., Zuo, T., McEachran, R. P., and Stauffer, A. D. (1992). *J. Phys. B* **25**, 3709.
- Trajmar, S., Williams, W., and Srivastava, S. K. (1977). *J. Phys. B* **10**, 3323.
- Zohny, E. I. M., El-Fayoumi, M. A. K., Hamdy, H., Beyer, H.-J., Eid, Y., Shahin, F., and Kleinpoppen, H. (1989). Contributed Papers to XVI ICPEAC (New York) (Eds A. Dalgarno *et al.*, p. 173.